



# On the protection of extrasolar Earth-like planets around K/M stars against galactic cosmic rays

J.-M. Grießmeier<sup>a,b,\*</sup>, A. Stadelmann<sup>c</sup>, J.L. Grenfell<sup>d,e</sup>, H. Lammer<sup>f</sup>, U. Motschmann<sup>c</sup>

<sup>a</sup> Laboratoire d'Etudes Spatiales et d'Instrumentation en Astrophysique (LESIA), Observatoire de Paris, CNRS, UPMC, Université Paris Diderot, 5 Place Jules Janssen, 92190 Meudon, France

<sup>b</sup> Netherlands Institute for Radio Astronomy, Postbus 2, 7990 AA, Dwingeloo, The Netherlands

<sup>c</sup> Technische Universität Braunschweig, Mendelssohnstraße 3, 38106 Braunschweig, Germany

<sup>d</sup> Institut für Planetenforschung, Deutsches Zentrum für Luft- und Raumfahrt (DLR), Rutherford Str. 2, 12489 Berlin, Germany

<sup>e</sup> Zentrum für Astronomie und Astrophysik, Technische Universität Berlin (TUB), Hardenbergstr. 36, 10623 Berlin, Germany

<sup>f</sup> Space Research Institute, Austrian Academy of Sciences, Schmiedlstr. 6, A-8042 Graz, Austria

## ARTICLE INFO

### Article history:

Received 5 February 2008

Revised 20 August 2008

Accepted 20 September 2008

Available online 12 November 2008

### Keywords:

Extrasolar planets

Cosmic rays

Magnetospheres

## ABSTRACT

Previous studies have shown that extrasolar Earth-like planets in close-in habitable zones around M-stars are weakly protected against galactic cosmic rays (GCRs), leading to a strongly increased particle flux to the top of the planetary atmosphere. Two main effects were held responsible for the weak shielding of such an exoplanet: (a) For a close-in planet, the planetary magnetic moment is strongly reduced by tidal locking. Therefore, such a close-in extrasolar planet is not protected by an extended magnetosphere. (b) The small orbital distance of the planet exposes it to a much denser stellar wind than that prevailing at larger orbital distances. This dense stellar wind leads to additional compression of the magnetosphere, which can further reduce the shielding efficiency against GCRs. In this work, we analyse and compare the effect of (a) and (b), showing that the stellar wind variation with orbital distance has little influence on the cosmic ray shielding. Instead, the weak shielding of M star planets can be attributed to their small magnetic moment. We further analyse how the planetary mass and composition influence the planetary magnetic moment, and thus modify the cosmic ray shielding efficiency. We show that more massive planets are not necessarily better protected against galactic cosmic rays, but that the planetary bulk composition can play an important role.

© 2008 Elsevier Inc. All rights reserved.

## 1. Introduction

One of the many fascinating questions in the field of exoplanet studies is the search for habitable worlds. Because of their relatively small mass, low luminosity, long lifetime and large abundance in the galaxy, M dwarfs are sometimes suggested as prime targets in searches for terrestrial habitable planets (Tarter et al., 2007; Scalo et al., 2007). The detection of planets with  $M \leq 10M_E$ , i.e. with a mass smaller than 10 terrestrial masses (the upper limit for “super-Earths” in the classification of Valencia et al., 2007) recently became possible with current advances in instrumentation and analysis. The first super-Earth detected was GJ 876d, a planet with  $\sim 7.5M_E$  orbiting an M star (Rivera et al., 2005). Thereafter, other low-mass planets have been discovered: OGLE-2005-BLG-390Lb, a planet with  $5.5M_E$  in an orbit of 5 AU was found by microlensing (Beaulieu et al., 2006), and HD 69830b, a planet with a minimum mass of  $10.2M_E$  in an orbit of 0.08 AU was detected by

the radial velocity technique (Lovis et al., 2006). More recently, two super-Earth planets were discovered around the M3 dwarf Gl 581, with minimum masses of  $5.0M_E$  and  $7.7M_E$ , and semimajor axes of 0.07 and 0.25 AU (Udry et al., 2007), and Ribas et al. (2008) report the possible detection of a  $5.0M_E$  planet around the M-type star GJ 436. In total, 6 planets with masses  $\lesssim 10M_E$  are known today, 5 of which are located in an orbit around an M star.<sup>1</sup> The least massive planet has a mass of  $5.0M_E$ . While the number of super-Earth planets around M stars is currently still limited, the detection of cold debris disks around M stars seems to indicate that planets may be as frequent for M stars as they are for F, G and K stars (Lestrade et al., 2006).

For M stars the habitable zone (defined by the range of orbital distances over which liquid water is possible on the planetary surface, see e.g. Kasting et al., 1993) is much closer to the star (depending on stellar mass, but typically  $\leq 0.3$  AU). Such close-in distances pose additional problems and constraints to habitability. For example, there is the possibility that the atmosphere might

\* Corresponding author at: Netherlands Institute for Radio Astronomy, Postbus 2, 7990 AA, Dwingeloo, The Netherlands.

E-mail address: griessmeier@astron.nl (J.-M. Grießmeier).

<sup>1</sup> Up-to-date numbers can be found at the Extrasolar Planets Encyclopaedia: <http://www.exoplanet.eu>.

collapse on the night side of the planet, although it seems that this problem is less severe than previously assumed (Joshi et al., 1997; Joshi, 2003). Intense stellar flares are common, especially for young M stars, but the radiation can be shielded by the planetary atmosphere (Heath et al., 1999). Both direct UV radiation (Buccino et al., 2007) and indirect UV radiation generated by energetic particles (Smith et al., 2004) can have important consequences for biogenic processes on M-star planets. Another potential problem for M star planet habitability is that one expects a large number of coronal mass ejections (CMEs) on active M stars. The related interaction of the dense CME plasma flux with the atmosphere/magnetosphere environment of the exposed planets during the active stage of the stellar evolution could be strong enough to erode the atmosphere or the planetary water inventory via non-thermal atmospheric loss processes (Khodachenko et al., 2007; Lammer et al., 2007).

The efficient loss of water from the planet could also lead to a breakdown of plate tectonics. If the majority of the planets' water is lost, the lithosphere will not be sufficiently deformable, and subduction of the crust cannot occur. The recycling of the crust through plate tectonics keeps the crust thin. If the crust is too thick, the lithospheric plate comprising the crust will be too buoyant to be subducted. A thin crust and a wet planet seem to be very important for plate tectonics to operate. Plate tectonics, however, help to cool the interior efficiently which is required to keep an Earth-like thermally driven magnetic dynamo in operation over geological time spans (Lammer et al., 2008). Even in the case of M star planets with a magnetic dynamo, the magnetic moment is not likely to be large. Terrestrial planets in the habitable zones of M-stars can be expected to be tidally locked, which leads to a reduction in the planetary magnetic moment (Grießmeier et al., 2005b). For these reasons, one can assume that M-star planets within the habitable zones are only weakly protected by their magnetospheres, resulting in a higher cosmic ray exposure. In addition, the small orbital distances of these planets expose them to much denser stellar winds than at larger orbital distances. The dense stellar winds lead to a further compression of the magnetospheres, which can in principle again reduce the shielding efficiency against GCRs.

In this work we extend the studies of Grießmeier et al. (2005b) and Grießmeier et al. (2005a) by separately quantifying and comparing these two effects (effect of enhanced stellar wind ram pressure due to the smaller orbital distance vs influence of a reduced planetary magnetic dipole moment). We show that the stellar wind variation with orbital distance has little influence on the shielding efficiency against galactic cosmic rays. The weak shielding found for M star planets (Grießmeier et al., 2005b, 2005a) thus has to be attributed to their reduced magnetic moment. Given that the magnetic moment is the key parameter, we further analyse the influence of the planetary mass and its composition on the planetary magnetic moment, and thus on the cosmic ray shielding efficiency.

This paper is organised as follows: The planetary parameters governing the size of the magnetosphere are presented in Section 2. We show that planets within the habitable zone of M stars are tidally locked, which leads to a reduced planetary magnetic dipole moment (Section 2.2). The stellar wind parameters at close orbital distances are discussed in Section 2.3. The influence of tidal locking and stellar wind on the size of the planetary magnetosphere is briefly mentioned in Section 2.4. In Section 2.5, we discuss the dependence of the cosmic ray flux *outside* the planetary magnetosphere on the orbital distance. The cosmic ray model (*inside* the magnetosphere) is explained in Section 3. In Section 4, the resulting flux of galactic cosmic rays to the atmospheres of different extrasolar planets is discussed. We study the effect of orbital distance via the stellar wind parameters (Section 4.1), tidal locking (Section 4.2), planetary mass and planetary composition

(Section 4.3). Potential implications are briefly discussed in Section 5. Section 6 closes with some concluding remarks.

## 2. The planetary situation

### 2.1. Tidal locking

Tidal locking (i.e. the synchronisation of the planetary rotation period to the planetary orbital period) occurs for planets orbiting very close to their parent star. The relevance of this process for terrestrial extrasolar planets is discussed in this section. This is an update to the corresponding section of Grießmeier et al. (2005b).

A planet with angular velocity  $\omega_i$  at  $t = 0$  (i.e. after formation) will gradually lose angular momentum, until the angular velocity reaches a constant value  $\omega_f$  at  $t = \tau_{\text{sync}}$ . For a planet with a mass of  $M_p$  and radius of  $R_p$  around a star of mass  $M_*$ ,  $\tau_{\text{sync}}$  can be expressed as (e.g. Murray and Dermott, 1999; Grießmeier et al., 2007, Appendix B):

$$\tau_{\text{sync}} \approx \frac{4}{9} \alpha Q'_p \left( \frac{R_p^3}{GM_p} \right) (\omega_i - \omega_f) \left( \frac{M_p}{M_*} \right)^2 \left( \frac{d}{R_p} \right)^6. \quad (1)$$

The parameters  $\alpha$ ,  $Q'_p$ ,  $\omega_i$  and  $\omega_f$  required to calculate the timescale for tidal locking of a terrestrial planet are presented further below.

Equation (1) shows that the timescale for tidal locking strongly depends on the distance ( $\tau_{\text{sync}} \propto d^6$ ). Thus, a planet in a close-in orbit around its central star is subject to strong tidal interaction, leading to gravitational locking on a very short timescale. Other important factors for the tidal locking timescale are the stellar mass and the planetary structure.

#### 2.1.1. Structure parameter $\alpha$

The constant  $\alpha$  depends on the internal mass distribution within the planet. It is defined by  $\alpha = I/(M_p R_p^2)$ , where  $I$  is the planetary moment of inertia. For a sphere of homogeneous density,  $\alpha$  is equal to 2/5. For planets, generally  $\alpha \leq 2/5$ . For the Earth, the structure parameter  $\alpha$  is given by  $\alpha = 1/3$  (Goldreich and Soter, 1966). In the following, this value will be used.

#### 2.1.2. Tidal dissipation factor $Q'_p$

$Q'_p$  is the modified  $Q$ -value of the planet. It is defined by (Murray and Dermott, 1999)

$$Q'_p = \frac{3Q_p}{2k_{2,p}}, \quad (2)$$

where  $k_{2,p}$  is the Love number of the planet.  $Q_p$  is the planetary tidal dissipation factor (the larger it is, the smaller is the tidal dissipation), defined by MacDonald (1964) and Goldreich and Soter (1966).

We use  $k_{2,p} = 0.3$  for the Earth (MacDonald, 1964; Murray and Dermott, 1999). This value will also be used for the “small super-Earth” and the “Ocean Planet” case. For the Earth, a value of  $Q_p \approx 12$  can be determined from the measured secular acceleration of the moon (Goldreich and Soter, 1966; Murray and Dermott, 1999). This value is relatively small when compared to other terrestrial planets, where  $Q_p$  is typically of the order of  $10^2$ . This is probably due to the fact that, for the Earth, much energy is dissipated in the shallow seas (MacDonald, 1964; Hubbard, 1984; Kasting et al., 1993; Murray and Dermott, 1999). In the past, when the continents were joined, the value of  $Q_p$  was probably larger (Peale, 1999; Murray and Dermott, 1999). For the case of the “small super-Earth” and the “Ocean Planet” (see below),  $Q_p$  is set to the value usually assumed for Venus and Mercury ( $Q_p \approx 100$ , Murray and Dermott, 1999).

From  $k_{2,p}$  and  $Q_p$ , the required value of  $Q'_p$  can be obtained using Eq. (2). We find  $Q'_p = 60$  for Earth and  $Q'_p = 500$  for both the “small super-Earth” and “Ocean Planet” cases.

### 2.1.3. Initial rotation rate $\omega_i$

The initial rotation rate  $\omega_i$  of a terrestrial planet is a poorly known quantity (see, e.g. Correia and Laskar, 2003). It certainly depends on the details of the planetary formation and can be strongly influenced by processes like migration or impacts. Therefore, two limits for  $\omega_i$  are considered:

- A relatively high initial rotation rate as suggested for the early Earth–Moon system, with  $\omega_i = 1.83\omega_E$  (with the current rotation period of the Earth  $\omega_E = 7.27 \times 10^{-5} \text{ s}^{-1}$ ) corresponding to a length of day of 13.1 h (MacDonald, 1964).
- A lower rotation rate with  $\omega_i = 0.80\omega_E$  corresponding to a day of 30 h.

Note that a primordial rotation period of the order of 10 h is consistent with the relation between the planetary angular momentum density and planetary mass observed in the Solar System (Hubbard, 1984, Chapter 4).

### 2.1.4. Final rotation rate $\omega_f$

As far as Eq. (1) is concerned, the final rotation rate  $\omega_f$  can be neglected, at least for the planets of interest in this work (Grießmeier, 2006).

### 2.1.5. Tidal locking: Results for exoplanets

Equation (1) allows us to calculate the timescale for tidal locking for terrestrial exoplanets. Subsequently, the planets can be classified as either “tidally locked,” “potentially tidally locked” or “unlocked.” The upper and lower boundaries of the potentially locked region are determined by the conditions  $\tau_{\text{sync}} = 100 \text{ Myr}$  and  $\tau_{\text{sync}} = 10 \text{ Gyr}$ , respectively. To account for the uncertainty of the initial rotation rate  $\omega_i$ , the lower boundary is calculated with  $\omega_i = 1.83\omega_E$  (i.e. a rotation period of 13.1 h), and the upper boundary is calculated with  $\omega_i = 0.80\omega_E$  (corresponding to a rotation period of 30 h). This increases the area of the “potentially locked” region.

In Fig. 1 (updated from Grießmeier et al., 2005b), the grey-shaded area gives the location of the continuously habitable zone (CHZ) according to Kasting et al. (1993). The lines delimit different parameter regimes for an Earth-like planet: All planets to the right of the dashed line are considered as tidally locked while planets to the left of the solid line are supposed to be freely rotating. One can see that all Earth-like planets inside the CHZ of M stars can be considered to be tidally locked.

In addition to the current Earth, two additional configurations are examined:

- The “small super-Earth” case (described in more detail in Section 4) is depicted in Fig. 2. It can be seen that the larger value of  $Q_p'$  slightly decreases the “tidally locked” regime.
- The “Ocean Planet” case (described in more detail in Section 4) is depicted in Fig. 3, with similar results than for the “small super-Earth” case.

As a typical test case, a terrestrial exoplanet at an orbital distance of 0.2 AU around a star of  $0.5M_\odot$  will be studied. Figs. 1–3 clearly show that such a planet, regardless of its precise mass, radius, and composition, is very likely to be tidally locked. The reduced rotation rate of tidally locked planets is supposed to have important consequences for the planetary magnetic dipole moment, which is discussed in Section 2.2.

## 2.2. Planetary magnetic moment

The planetary magnetic dipole moment can be estimated from different scaling laws (Grießmeier et al., 2005b). It can be shown

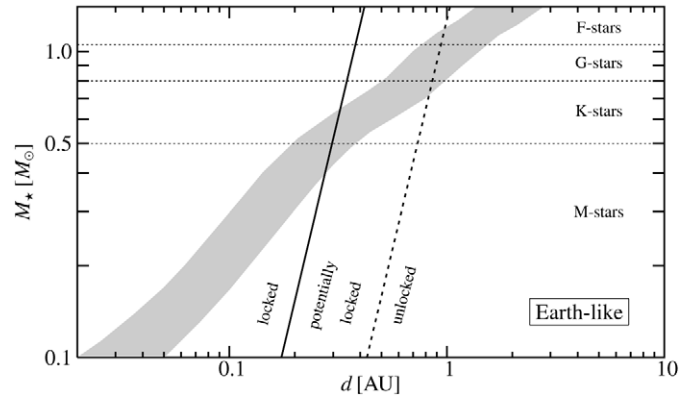


Fig. 1. Tidally locked (left) vs freely rotating (right) regime for Earth-like planets as a function of orbital distance  $d$  and mass  $M_*$  of the host star. The shaded area gives the location of the continuously habitable zone (CHZ). Updated from Grießmeier et al. (2005b).

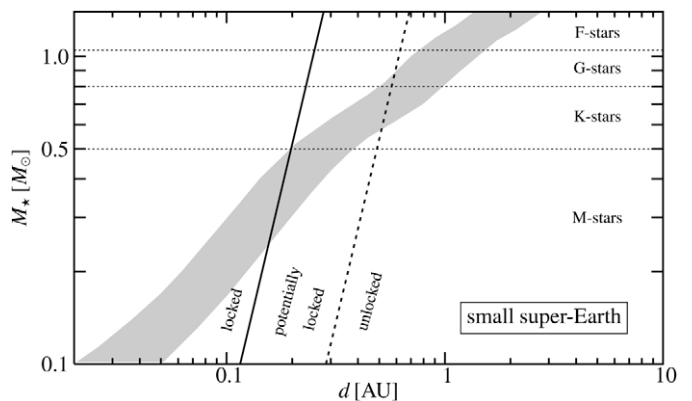


Fig. 2. Tidally locked (left) vs freely rotating (right) regime for a “small super-Earth” as a function of orbital distance  $d$  and mass  $M_*$  of the host star. The shaded area gives the location of the continuously habitable zone (CHZ).

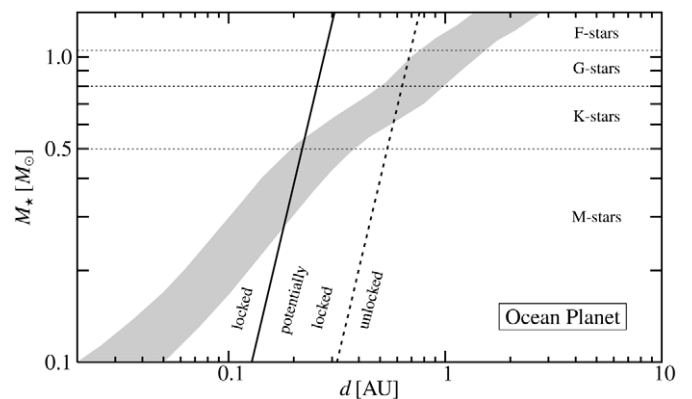


Fig. 3. Tidally locked (left) vs freely rotating (right) regime for an “Ocean Planet” as a function of orbital distance  $d$  and mass  $M_*$  of the host star. The shaded area gives the location of the continuously habitable zone (CHZ).

that for the slowly rotating tidally locked planets, the magnetic moment is much smaller than for freely rotating planets. For an Earth-like planet in an orbit of 0.2 AU around a star with 0.5 stellar masses, the magnetic moment is expected to lie in the range  $0.02\mathcal{M}_E < \mathcal{M} < 0.15\mathcal{M}_E$ , where  $\mathcal{M}_E$  is the value of Earth’s current magnetic moment (Grießmeier et al., 2005b). In the following, the maximum value of  $0.15\mathcal{M}_E$  will be adopted to obtain a lower limit for the cosmic ray flux to the atmosphere. Magnetic moments resulting for a few other configurations are given in Table 1.

**Table 1**

Parameters for the different planetary configurations.  $d$ : orbital distance,  $M_*$ : stellar mass,  $\mathcal{M}$ : planetary magnetic moment,  $R_s$ : standoff distance,  $B$ : magnetic field at the magnetopause.

Planet	$d$ [AU]	$M_*$ [ $M_\odot$ ]	$\mathcal{M}$ [ $\mathcal{M}_E$ ]	$R_s$ [ $R_p$ ]	$B(R_s)$ [nT]
Case 1: Unmagnetised	Any	Any	0	–	–
Case 2: (Unlocked) Earth	1.0	1.0	1.0	9.91	73
Case 3: Locked exoplanet	0.2	0.5	0.15	4.12	150
Case 4: (Hyp.) unlocked exoplanet	0.2	0.5	1.0	7.81	150
Case 5: (Hyp.) locked Earth	1.0	1.0	0.15	5.23	73
Case 6: Small super-Earth ( $6M_E$ )	0.2	0.5	0.65	4.15	150
Case 7: Large super-Earth ( $10M_E$ )	0.2	0.5	0.96	4.13	150
Case 8: Ocean Planet	0.2	0.5	0.37	2.80	150

### 2.3. Stellar wind

It is known that at the close orbital distances of M-star habitable zones the stellar wind has not yet reached the quasi-asymptotic velocity regime. Because of the low stellar wind velocity, the planetary magnetosphere is less strongly compressed at such distances than one would expect from stellar wind models with a constant velocity. To capture this behaviour realistically and to correctly describe the flux of galactic cosmic rays into the atmospheres of close-in exoplanets, we require a model with a radially dependent stellar wind velocity.

For slowly rotating stars, the stellar wind may be described by the solution of the purely hydrodynamic, isothermal model of Parker (1958). In this model, the interplay between stellar gravitation and pressure gradients leads to a supersonic flow for sufficiently large substellar distances  $d$  (see e.g. Parker, 1958; Mann et al., 1999; Pröls, 2004). In accordance with the observations, this model describes a solar wind with low velocity and large acceleration near the Sun, whereas at larger distances the velocity is large and the acceleration strongly decreases.

The procedure to obtain the stellar wind velocity  $v_{\text{eff}}(d, M_*, R_*)$  and density  $n(d, M_*, R_*)$  at the location of an exoplanet (i.e. at distance  $d$ ) for a host star of given mass  $M_*$ , and radius  $R_*$  consists of the following:

- (1) The stellar mass loss rate is assumed to be proportional to its surface area:

$$\dot{M}_* = \dot{M}_\odot \frac{R_*^2}{R_\odot^2}, \quad (3)$$

where the subscripts  $\odot$  and  $*$  denote solar and stellar properties, respectively.

- (2) A Parker-like stellar wind model is used to find  $n(d)$  and  $v(d)$  as a function of the distance to the star. The coronal temperature  $T_{\text{corona}}$  is adjusted until the stellar wind velocity at 1 AU corresponds to the value which was obtained in step 1. With this value of  $T_{\text{corona}}$ ,  $v$  can be determined for any value of  $d$  by solving Parker's wind equation. Thus,  $v(d)$  is obtained.
- (3) Because of  $\dot{M}_* = 4\pi d^2 n(d) v(d) m$  (where  $m$  is the proton mass), the density  $n(d)$  is obtained by dividing the stellar mass loss  $\dot{M}_*$  obtained in step 1 by  $4\pi d^2 v(d) m$ , where  $v(d)$  was obtained in step 2.
- (4) The effective stellar wind velocity relative to the planet  $v_{\text{eff}}$  is calculated from  $v$  (as obtained in step 2 above) and the planetary orbital velocity ( $v_{\text{eff}} = \sqrt{v^2 + v_{\text{orbit}}^2}$ ).

This procedure is similar to that of Grießmeier et al. (2005b), with the difference that here we keep the stellar age fixed (at 4.6 Gyr) to compare stars of identical ages.

### 2.4. Magnetospheric model

The magnetosphere is modelled as a cylinder topped by a half-sphere (Voigt, 1981; Stadelmann, 2005; Grießmeier et al., 2005b). A closed magnetosphere is assumed, i.e. field lines are not allowed to pass through the magnetopause. Within this model, the magnetic field is defined for any point inside the magnetosphere as soon as the planetary magnetic moment and the size of the magnetosphere are prescribed. The size of the magnetosphere is characterised by the magnetopause standoff distance  $R_s$ , i.e. the extent of the magnetosphere along the line connecting the star and the planet.  $R_s$  can be obtained from the pressure equilibrium at the substellar point. This pressure balance includes the stellar wind ram pressure, the stellar wind thermal pressure of electrons and protons, and the planetary magnetic field pressure:

$$mnv_{\text{eff}}^2 + 2nk_B T = \frac{\mu_0 f_0^2 \mathcal{M}^2}{8\pi^2 R_s^6}. \quad (4)$$

Here,  $f_0 = 1.16$  is the form factor of the magnetosphere and includes the magnetic field caused by the currents flowing on the magnetopause (Voigt, 1995; Grießmeier et al., 2004).  $\mathcal{M}$  is the planetary magnetic dipole moment as discussed in Section 2.2.

For a given planetary orbital distance  $d$ , only the magnetospheric magnetic pressure is a function of the distance to the planet, while the other contributions are constant. Thus, from the pressure equilibrium Eq. (4) the standoff distance  $R_s$  is found to be:

$$R_s = \left[ \frac{\mu_0 f_0^2 \mathcal{M}^2}{8\pi^2 (mnv_{\text{eff}}^2 + 2nk_B T)} \right]^{1/6}. \quad (5)$$

Table 1 lists the standoff distances  $R_s$  (in planetary radii  $R_p$ ) for different planetary configurations as well as the magnetic field strength at the location of the magnetopause,  $B(R_s)$ .

### 2.5. Cosmic ray flux outside the magnetosphere as a function of orbital distance

In the Solar System, the cosmic ray flux is known to increase with increasing heliocentric distance. This is attributed to effects such as diffusion, convection, adiabatic deceleration as well as gradient and curvature drifts (see, e.g. Kallenrode, 2000; Heber et al., 2006). The theoretical basis for this approach is described by Fichtner (2001, Section 2.3). In this section, we study how strong such effects are in the inner heliosphere to see how much smaller the cosmic ray flux outside the magnetosphere of a close-in exoplanet (e.g. at 0.2 AU) may be compared to one in an Earth-like orbit. The penetration of these particles through the planetary magnetosphere is described in Section 4.

The radial gradient of the cosmic ray intensity  $J$  depends on the heliocentric distance  $d$ . Between 1 and 42 AU, McDonald et al. (1992) approximate it by:

$$\frac{1}{J} \frac{dJ}{dd} = G_0 \left( \frac{d_e}{d} \right)^\alpha. \quad (6)$$

During solar minimum,  $\alpha \approx 0.7$  for cosmic ray protons (the exact value depends on the particle energy), and  $G_0 \approx 0.2 \text{ AU}^{-1}$ . The orbital distance of the Earth is denoted by  $d_e = 1 \text{ AU}$ .

Equation (6) is equivalent to a relative cosmic ray flux of:

$$J_{\text{rel}}(d) = J_0 \exp \left[ G_0 (d^{1-\alpha}) \frac{d_e^\alpha}{1-\alpha} \right], \quad (7)$$

where  $J_0$  is determined by the condition  $J_{\text{rel}}(d_e) = 1$ . Fig. 4 shows  $J_{\text{rel}}(d)$ .

With this, we can compare the cosmic ray flux at different distances. We find that  $J(0.2 \text{ AU}) \approx 0.8 \cdot J(1.0 \text{ AU})$ , and  $J(40 \text{ AU}) \approx$

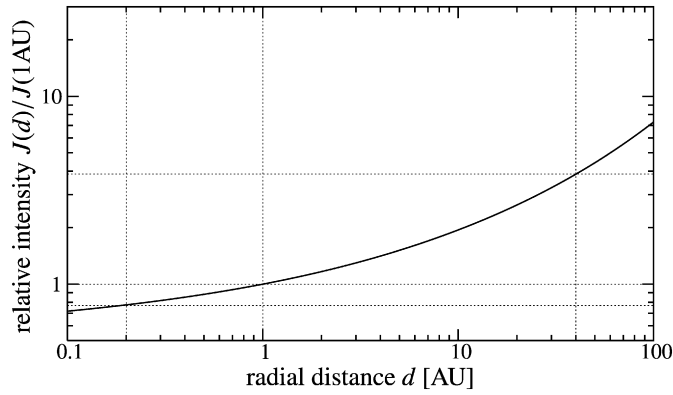


Fig. 4. Relative cosmic ray flux in the heliosphere as a function of heliocentric distance.

$4 \times J(1.0 \text{ AU})$ . For distances below 1.0 AU, the particle flux varies only weakly, so that we can neglect this effect when calculating fluxes of cosmic rays into the atmospheres of close-in planets.

Note that the radial gradient could be different for other stars than in the Solar System. For a low mass  $M$  star with a lower stellar wind density, we would expect the radial gradient of the cosmic ray intensity to be smaller, whereas it is likely to be larger for a star with a denser and faster stellar wind (as would be the case, e.g. for a younger star, see Wood et al., 2002, 2005; Grießmeier et al., 2005b; Holzwarth and Jardine, 2007). While a quantitative computation of the cosmic ray gradients around other stars would be interesting, this is outside the scope of this paper. This question will be addressed in the future. For the moment, we will assume that the cosmic ray modulation around other stars is not much larger than that found in the Solar System, and we will correspondingly neglect it in the remainder of this work.

### 3. Cosmic ray protection

In order to quantify the protection of extrasolar Earth-like planets against galactic cosmic rays, the motion of galactic cosmic protons through planetary magnetospheres is investigated numerically.

#### 3.1. Cosmic ray calculation

In order to determine the impact of GCR protons in the energy range  $64 \text{ MeV} < E < 8 \text{ GeV}$  on the planetary atmosphere, particle trajectories in the magnetosphere are analysed. Because no solution in closed form exists, this is only possible through the numerical integration of many individual trajectories (Smart et al., 2000). For each particle energy (64 MeV, 128 MeV, 256 MeV, 512 MeV, 1024 MeV, 2048 MeV, 4096 MeV and 8192 MeV) and for each magnetospheric configuration, over 7 million trajectories are calculated, which correspond to protons with different starting positions and starting velocity directions. The particles are launched from the surface of a sphere centred on the planet. The radius of this sphere satisfies the condition  $r \geq R_s$ , so that the particles are launched outside the magnetosphere (except for those arriving from the tailward direction).

Once the particles enter the magnetosphere, their motion is influenced by the planetary magnetic field. This magnetic field is calculated from the magnetospheric model of Section 2.4. Note that Table 1 gives the *maximum* values for the planetary magnetic moments. For this reason, the results represent the lower limit for the cosmic ray flux to the atmosphere. For a smaller magnetic moment, a larger cosmic ray flux is possible. The trajectories are calculated using the numerical leapfrog method. For each energy, all particles are counted which reach the atmosphere (described

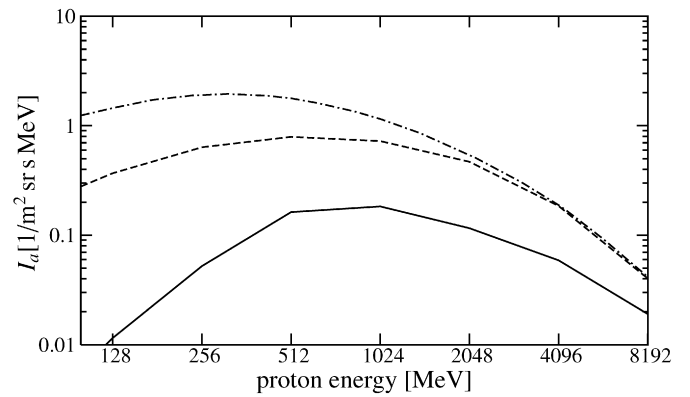


Fig. 5. Dash-dotted line: energy spectrum outside the magnetosphere, according to Seo et al. (1994). Dashed line: energy spectrum of cosmic ray protons impacting the atmosphere (100 km above the surface) of an Earth-like planet at 0.2 AU around a  $0.5M_{\odot}$  K/M star. Solid line: energy spectrum of cosmic rays impacting the atmosphere of the Earth. From Grießmeier et al. (2005b).

by a spherical shell one hundred kilometres above the planetary surface, i.e.  $R_a = R_p + 100 \text{ km}$ ). The impact of particles on the planetary atmosphere is quantified by the energy spectrum, which is defined in Section 3.2. More details on the numerical calculation of the cosmic rays trajectories can be found in Stadelmann (2005).

Note that for the planetary system we implicitly assume an environment similar to that of the solar neighbourhood. Planets in other regions of the galaxy (e.g. those encountering a different interstellar medium, or those close to the galactic centre) may be subject to very different cosmic ray fluxes (e.g. Scherer et al., 2008).

#### 3.2. Cosmic ray energy spectrum

The cosmic ray *energy spectrum* is determined in the following way: for a given particle energy, the fraction of particles reaching the planetary atmosphere is registered. This value is compared to the fraction of particles reaching the atmosphere of an identical, but unmagnetised planet. The resulting magnetospheric filter function is multiplied with the cosmic ray energy spectrum outside the magnetosphere, which was taken from Seo et al. (1994). Fig. 5 shows the reference energy spectrum of Seo et al. (1994) as a dash-dotted line. The energy spectrum on top of the Earth's atmosphere is shown as a solid line, whereas the dashed line corresponds to the cosmic ray energy spectrum for an Earth-like exoplanet in an orbit of 0.2 AU around a  $0.5M_{\odot}$  K/M star.

### 4. Comparison of GCR fluxes for eight scenarios

In the following, the flux of cosmic rays at the top of the atmosphere will be compared for eight different planetary configurations. The energy spectrum is determined for the following cases:

- Case 1: “Unmagnetised case.” This is the (reference) cosmic ray energy spectrum outside any planetary magnetosphere (interplanetary case, taken from Seo et al., 1994). At the same time, this corresponds to the flux arriving at the top of the atmosphere of a totally unmagnetised planet (i.e. without even induced magnetic fields). This case is valid for any stellar mass. In the following figures, it is represented by a dash-dotted line.
- Case 2: “(Unlocked) Earth case.” The case of the magnetosphere of today's Earth (i.e. at 1.0 AU of a Sun-like star with  $M_{\star} = 1.0M_{\odot}$ ). The Earth's magnetic field is represented by a zonal dipole with a Gaussian coefficient of  $g_{10} = 31 \mu\text{T}$ . In all figures, this case is represented by a solid line.

- Case 3: “Locked exoplanet case.” The case of the magnetosphere of an extrasolar planet in an orbit of 0.2 AU around an K/M star of 0.5 solar masses. Due to tidal locking, the magnetic moment is reduced to 15% of the Earth’s magnetic moment (see Section 2.2). For this situation, a dashed line is used.
- Case 4: (Hypothetical) “unlocked exoplanet case.” Identical to the “locked exoplanet case” (e.g. located at 0.2 AU around a Sun-like star with  $M_\star = 0.5M_\odot$ ), with the only difference being the magnetic moment: Here we assume that the planet is *not* tidally locked and has a strong magnetic moment ( $\mathcal{M} = 1.0\mathcal{M}_E$ ). Note that this case is not realistic (unless the planet was brought to this position only recently), but it is instructive to compare the influence of the stellar proximity and the small planetary magnetic moment. In the figures, this case will be shown by filled triangles.
- Case 5: (Hypothetical) “locked Earth case.” Identical to the “(unlocked) Earth case” (e.g. at 1.0 AU distance from a Sun-like star with  $M_\star = 1.0M_\odot$ ), but assuming that the planet only has a small magnetic moment ( $\mathcal{M} = 0.15\mathcal{M}_E$ ). This case can also be seen as a “weakly magnetised Earth case.” Similarly to the “unlocked exoplanet case,” this case will be used to disentangle the effect of stellar proximity and of small magnetic moment. For this case, circles are used.
- Case 6: “Small super-Earth case” (6 Earth masses, 1.63 Earth radii, as modelled by Léger et al., 2004). Similar to the “locked exoplanet case” (case 3), but for a large terrestrial exoplanet, assuming tidal locking. As was mentioned before, the first planets of such size have now been detected. This case is represented by a double-dashed line.
- Case 7: “Large super-Earth case” (10 Earth masses, 1.86 Earth radii, making use of the scaling relations of Valencia et al., 2006). Similar to the “locked exoplanet case” (case 3) or the “small super-Earth case” (case 6), but for a larger planetary mass, assuming tidal locking. This planet is denoted by a triple-dashed line. Together with the “locked exoplanet case” and the “small super-Earth case,” this will be used to analyse the dependence of cosmic ray protection on the planetary mass.
- Case 8: “Ocean Planet case” (6 Earth masses, 2.0 Earth radii, as modelled by Léger et al., 2004). Similar to the “Small super-Earth case” (case 6), but for an Ocean Planet (i.e. a planet with a significant fraction of water ice, see e.g. Kuchner, 2003; Léger et al., 2004; Selsis et al., 2007). For this situation, a dotted line is used.

For each of the above cases, the input parameters (the orbital distance  $d$  and the stellar mass  $M_\star$ ) and the resulting values (the magnetic moment  $\mathcal{M}$ , the standoff distance  $R_s$  and the magnetic field strength at the magnetopause  $B(R_s)$ ) are given in Table 1. The stellar mass has two functions: It determines the rotation rate of tidally locked planets (case 3 and cases 5–8), and it defines the stellar wind flux onto the magnetosphere, thus defining the size of the magnetosphere via Eq. (3). For case 1 (no magnetosphere), the stellar mass does not matter. As noted before, the magnetic moments (and thus also the standoff distances) are assumed to have the maximum allowed value. Thus the values obtained in this section represent a lower limit for the flux of cosmic ray protons to the planetary atmosphere. Table 1 also includes the magnetic field strength at the magnetopause. By definition of the magnetic moment,  $B(R_s) \propto \mathcal{M}R_s^{-3}$ . When the contribution of the thermal pressure in Eq. (4) is negligible, this results in  $B(R_s) \propto \sqrt{nv_{\text{eff}}^2}$ , so that the magnetic field strength at the magnetopause is identical e.g. for cases 3 and 4, but different for case 5.

The cosmic ray flux to the planetary atmosphere depends also on the stellar age (which is a crucial parameter for the stellar wind

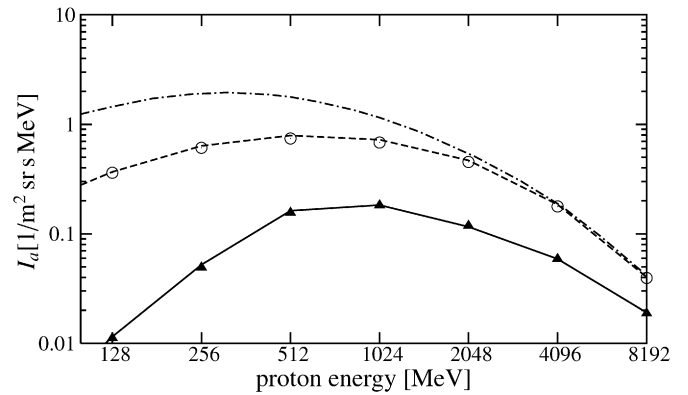


Fig. 6. Cosmic ray energy spectrum. Dash-dotted line: energy spectrum outside the magnetosphere (case 1, “unmagnetised case”). Dashed line: “locked exoplanet case” (case 3). Circles: hypothetical “locked Earth case” (case 5). Solid line: “(unlocked) Earth case” (case 2). Triangles: hypothetical “unlocked exoplanet case” (case 4).

velocity and density). This effect was discussed in Grießmeier et al. (2005b).

#### 4.1. Influence of orbital distance via the stellar wind parameters

Previously, the cosmic ray flux to the atmosphere of a tidally locked Earth-like exoplanet around a K/M type star with  $M_\star = 0.5M_\odot$  has been calculated (Grießmeier et al., 2005b). It was shown that such a planet (corresponding to our case 3) will be subject to very high cosmic ray fluxes when compared to the Earth (corresponding to our case 2). For particle energies below 200 MeV, the cosmic ray flux to the exoplanet was found to be up to one order of magnitude higher than on Earth, and for energies above 2 GeV magnetospheric shielding is negligible for the exoplanet case. This can also be seen in Fig. 5. As stated by Grießmeier et al. (2005b), two effects can contribute to this high cosmic ray flux: (a) the reduced planetary magnetic dipole moment due to tidal locking (Section 2.2) and (b) the enhanced stellar wind ram pressure at small orbital distances (Section 2.3). Both<sup>2</sup> contribute to the magnetospheric compression, which in turn determines the flux of high energy cosmic ray particles onto the planetary atmosphere. Here, we compare the relative importance of these two effects.

We first estimate the importance of the orbital distance via the stellar wind parameters. In Fig. 6, we first compare the cosmic ray energy spectra of the two strongly magnetised cases (with  $\mathcal{M} = 1.0\mathcal{M}_E$ ): The case of the Earth (case 2, solid line) and the hypothetical case of a strongly magnetised exoplanet (case 4, triangles). It can be seen that the cosmic ray energy spectra are identical at  $d = 1.0$  AU (case 2, solid line) and at  $d = 0.2$  AU (case 4, triangles). We also compare the two weakly magnetised cases (with  $\mathcal{M} = 0.15\mathcal{M}_E$ ): the weakly magnetised exoplanet case with  $d = 0.2$  AU (case 3, dashed line) and the hypothetical case of the weakly magnetised Earth at  $d = 1.0$  AU (case 5, circles). Again, despite the large difference in orbital distance (0.2 and 1.0 AU), Fig. 6 shows that the cosmic ray energy spectrum is identical for these two cases.

The distance-dependent stellar wind ram pressure does not seem to have any measurable influence on the cosmic ray energy spectrum. This may seem surprising, as it clearly has some influence on the size of the planetary magnetosphere, see Table 1 (col-

<sup>2</sup> In principle, a third effect plays a role, namely the stellar mass and radius, which determine the stellar wind (e.g. via Eq. (3)). However, if a solar mass star was used in case 3, the planetary magnetosphere would be even more compressed, which does not decrease the cosmic ray flux. Thus, the two other effects have to be responsible for the large difference in cosmic ray fluxes.

umn 5). However, Table 1, column 6 shows that the magnetic field at the magnetopause is *increased* when the orbital distance of a planet is decreased while keeping the magnetic moment constant. This directly results from the pressure balance in Eq. (4). Thus, when the orbital distance is decreased while the magnetic moment is kept fixed, the smaller size of the magnetosphere is compensated by a larger magnetic field at the magnetopause  $B(R_S)$ , which keeps the cosmic ray shielding at a constant level. In other words,  $R_S$ , the size of the planetary magnetosphere, is not a sufficient indicator for the quality of the magnetospheric shielding of a planetary atmosphere.

#### 4.2. Influence of tidal locking

If the difference of the cosmic ray energy spectra between a locked exoplanet and the Earth cannot be explained by the different orbital distances, the discrepancy lies in magnetic moment differences. This can be seen by comparing the cosmic ray energy spectrum of the Earth case (case 2, solid line) to the cosmic ray flux of a hypothetical Earth twin planet with a reduced magnetic moment (case 5, circles), with all other parameters kept constant ( $d = 1.0$  AU,  $M_* = 1.0M_\odot$ ). Fig. 6 shows that the energy spectrum is much higher in the weakly magnetised case ( $\mathcal{M} = 0.15\mathcal{M}_E$ , case 5, circles) than in the strongly magnetised case ( $\mathcal{M} = 1.0\mathcal{M}_E$ , case 2, solid line). We also compare the two exoplanet cases ( $d = 0.2$  AU,  $M_* = 0.5M_\odot$ ), namely the “locked exoplanet case” (case 3, dashed line) and the “unlocked exoplanet case” (case 4, triangles). Again, it can be seen that the cosmic ray energy spectrum has much higher values for the weakly magnetised case than in the strongly magnetised case. Obviously, the influence of tidal locking, hence the reduced magnetic moment (and not the stellar wind ram pressure) is the decisive factor for the increased influx of cosmic ray particles in case 3 (when compared to case 2). The similarity of cases 2 and 4 (and of cases 3 and 5) also shows that protons of the chosen energy range mostly feel the planetary dipole field, and that the field of the magnetopause currents has little influence (Vogt et al., 2007, Eq. (20)).

Similarly to a change in orbital distance, the planetary magnetic moment directly influences the size of the planetary magnetosphere (see Table 1, column 5). When the magnetic moment is changed, however, the magnetic field strength at the magnetopause (shown in Table 1, column 6) does not differ (compare cases 2 and 5, and cases 3 and 4, respectively). Thus, when  $B(R_S) = \text{const}$ , the quality of the magnetospheric shielding of the planetary atmospheres depends on the size of the magnetosphere  $R_S$ , i.e. it is weaker for those planets with a smaller magnetosphere.

We conclude that, of the two effects suggested by Grießmeier et al. (2005b), only one (namely the effect of tidal locking) has a measurable influence on the cosmic ray flux. The other effect (stellar wind density variation with orbital distance) appears to have negligible influence.

#### 4.3. Influence of planetary type

For planets with different size or composition than the Earth, the planetary magnetic dipole moment and the size of the magnetosphere are different from the Earth-like case. A few such cases are shown in Table 1 and discussed in this section.

Both “super-Earth” cases (cases 6 and 7) correspond to the case of a terrestrial planet with a composition similar to that of the Earth, but with higher planetary masses (6 and 10 Earth masses, respectively) and correspondingly larger radii (1.63 and 1.86 Earth radii, see the models of Léger et al., 2004, and Valencia et al., 2006). For both cases, the expected magnetic moment (Table 1, column 4) is larger than for an Earth-like planet (case 3). The larger magnetic moments lead to more extended magnetospheres

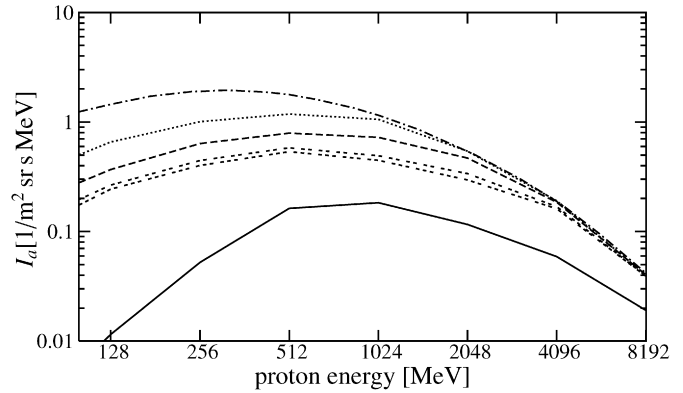


Fig. 7. Cosmic ray energy spectrum for different types of planets. Dash-dotted line: energy spectrum outside the magnetosphere (case 1, “unmagnetised case”). Dotted line: “Ocean Planet case” (case 8). Dashed line: Earth-like planet (case 3, “locked exoplanet case”). Double-dashed line: “small super-Earth case” (case 6). Triple-dashed line: “large super-Earth case” (case 7). Solid line: “(unlocked) Earth case” (case 2).

(Table 1, column 5). Because the planetary radius is larger, however, the planetary atmosphere is located at a larger distance from the planetary centre, so that the protection from galactic cosmic rays should not be expected to be much more efficient than for an Earth-like planet. Fig. 7 shows that this is indeed the case: The energy spectra of the “locked exoplanet case” (case 3, dashed line), of the “small super-Earth case” (case 6, double-dashed line) and of the “large super-Earth case” (case 7, triple-dashed line) are relatively similar. It can be seen that massive terrestrial planets do not necessarily have a much more efficient magnetospheric protection against galactic cosmic rays than an Earth-mass planet.

The “Ocean Planet case” (case 8, dotted line) corresponds to a planet with a different composition: 17% metals, 33% silicates, and 50% water ice (this corresponds to the Ocean Planet modelled by Léger et al., 2004). This change in composition reduces the average density when compared to the “super-Earth” case of the same mass: The radius of a 6 Earth-mass Ocean Planet is 2.0 Earth radii (as compared to the 1.63 Earth radii used above). This moves the atmosphere further away from the centre of the protecting dipole. Also, the reduced density leads to a somewhat reduced magnetic moment estimation. This is reflected in the small standoff distance measured in planetary radii (see Table 1) when compared to the “small super-Earth case” (case 6, double-dashed line), and the cosmic ray flux through the magnetosphere can be expected to be larger. These expectation is confirmed by the cosmic ray energy spectrum in Fig. 7. More cosmic ray particles reach the atmosphere for the “Ocean Planet case” (case 8, dotted line) than that of the “small super-Earth case” (case 6, double-dashed lines). Note that both planets have the same mass ( $6M_E$ ), so that the difference is caused only by the difference in composition. For energies above 100 MeV, the cosmic ray protection of an Ocean Planet (case 8) is weaker by a factor 2–3 than for a rocky planet of similar mass (case 6). We conclude that the planetary composition can be a potentially important factor concerning cosmic ray protection.

## 5. Implications

The increased flux of cosmic ray protons of galactic origin to the upper atmospheres of M-star planets has implications for the atmospheric composition and thus for the remote detection of biomarkers. It will also influence the flux of (secondary) cosmic ray particles reaching the ground, which can be expected to have biological implications.

### 5.1. Atmospheric implications

In the near future, atmospheres of extrasolar planets will be studied from the point of view of possible biological activity. “Atmospheric biomarkers” are compounds present in an atmosphere which imply the presence of life and which cannot be explained by inorganic chemistry alone. The simultaneous presence of significant amounts of atmospheric reducing gases (e.g. methane) and oxidising gases (e.g. oxygen) as on the Earth is also an indicator of biological activity (Lovell, 1965; Sagan et al., 1993). Good biomarkers include oxygen (produced by photosynthesis), ozone (mainly produced from oxygen) and nitrous oxide (produced almost exclusively from bacteria).

For the study of biomarkers in planetary atmospheres, it is important to know all inorganic effects which can modify the abundances of these molecules. Modelling studies (e.g. Schindler and Kasting, 2000; Selsis et al., 2002) are required to rule out false conclusions in cases where inorganic chemistry can mimic the presence of life. Grenfell et al. (2007b) looked at the response of biomarker chemistry on varying planetary parameters (e.g. orbital distance, stellar type). Here, we will discuss the response of biomarkers to cosmic rays.

The influence of a high flux of GCRs to the atmospheres of planets in the habitable zone (HZ) around M-stars was studied by Grenfell et al. (2007a). When cosmic rays travel through an Earth-like atmosphere, they have sufficient energy to break the strong  $N_2$  molecule and the chemical products react with oxygen to form nitrogen oxides ( $NO_x$ ). If UV levels are intense, e.g. corresponding to the upper mesosphere and above on the Earth, then the  $NO_x$  cannot survive.  $NO_x$  affects biomarkers differently depending on altitude. In a tropospheric environment, ozone is enhanced by  $NO_x$  due to the smog mechanism (Haagen-Smit, 1952). In a stratospheric environment, ozone is depleted by catalytic cycles (Crutzen, 1970). Once ozone is affected, the other biomarkers can change too, because ozone affects the temperature profile (hence e.g. mixing processes, chemical sources and sinks) and UV levels (hence photolysis rates) of other chemical species.

Using the cosmic ray spectra of our cases 1, 2 and 3, it was shown that GCRs may enhance the production of  $NO_x$  by a factor of three, which may modify the abundances of biomarker molecules (especially water and ozone) by up to 25% (Grenfell et al., 2007a).

It thus seems that most biomarkers are not strongly influenced by galactic cosmic rays for Earth-like planets in close orbits around M-stars. The case is different for solar energetic particles, which can strongly modify the abundance of ozone in the planetary atmosphere (Grenfell et al., 2008). Such changes in atmospheric biomarker concentrations have to be taken into account when searching for biosignatures in the spectra of Earth-like exoplanets (Selsis, 2004) by future space missions like DARWIN (Fridlund, 2004) or SEE-COAST (Schneider et al., 2006).

### 5.2. Biological implications

While a quantitative treatment is not yet available, the increased flux of cosmic rays at the top of the planetary atmosphere has not only implications for atmospheric chemistry and biomarkers, but also for the flux of secondary radiation on the surface. When galactic cosmic rays of sufficiently high energy reach the planetary atmosphere, they generate showers of secondary cosmic rays. Of the different components of such showers, slow neutrons have the strongest influence on biological systems. The propagation of high energy cosmic ray particles also depends on the composition and density of the planetary atmosphere. For an Earth-like atmosphere, the minimum energy which a proton must have to initiate a nuclear interaction that may be de-

tectable at sea level is approximately 450 MeV (Reeves et al., 1992; Shea and Smart, 2000). Terrestrial planets with dense atmospheres like Venus (100 bar surface pressure) would be better shielded by the planetary atmosphere, so that no secondary radiation can reach the surface. On the other hand, for planets with thin atmospheres like Mars (6 mbar surface pressure), the surface would probably be totally sterilised, even for a relatively low cosmic ray flux.

Keeping the atmospheric pressure constant at  $\sim 1$  bar, the flux at energies  $>450$  MeV is strongly increased for the planetary situations presented in Section 4 (see Figs. 6 and 7), and a large increase of secondary cosmic rays can be expected at the planetary surface.

Biological effects, namely an increase in cell fusion indices for different cell-lines, were found to be significantly correlated with the neutron count rate at the Earth’s surface (Belisheva et al., 2005; Grießmeier et al., 2005b). Similar, but much stronger and more diverse effects were observed during large solar particle events, where solar cosmic rays dominate over galactic cosmic rays. The effect of cosmic rays on cells and on DNA are potentially hazardous for life. On the other hand, changes at the genetic level are a necessary condition for biological evolution, so that cosmic rays may also play a role in radiation-induced evolutionary events.

As tidally locked Earth-like exoplanets inside the HZ of low-mass K/high-mass M stars are only weakly protected against high energetic cosmic rays, they can be expected to experience a higher surface neutron flux and stronger biological effects than Earth-like planets with a strong magnetic moment. For this reason, it may be more difficult for life to develop on the surface of planets around such stars. It was also shown (Section 4.3) that larger planets (super-Earths) are not much better protected against GCRs than smaller planets.

## 6. Conclusion

The atmospheres of extrasolar planets with orbits in the habitable zone of M stars are exposed to high fluxes of galactic cosmic rays. We have studied the effect of orbital distance via the stellar wind parameters, tidal locking, planetary mass and planetary composition on the cosmic ray fluxes. In previous works, the weak shielding found for M star planets was attributed to a combination of the enhanced stellar wind ram pressure with the reduced planetary magnetic dipole moment (Grießmeier et al., 2005b, 2005a). Here, we have shown that the variable stellar wind density at different orbital distance ranging from 0.2 to 1.0 AU (i.e. the CHZ of star with  $0.5M_{\odot} < M_{\star} < 1.0M_{\odot}$ ) has little influence on the GCR flux. The planetary magnetic moment is the decisive parameter: Tidally locked planets with a small magnetic moment have much higher particle fluxes than freely rotating planets with stronger magnetic moments.

We also find that more massive planets are not necessarily much better protected against galactic cosmic rays, but that the planetary composition can play an important role.

Generally speaking, to determine the magnetospheric shielding of a planetary atmosphere, it is not sufficient to calculate  $R_s$ , the size of the planetary magnetosphere, but one has also to take into account  $B(R_s)$ , the magnetic field at the magnetopause.

The above factors have to be considered for missions studying biosignatures in the spectra of Earth-like exoplanets for two reasons: The enhanced flux of galactic cosmic rays may naturally generate or destroy molecules typically regarded as biomarkers (Grenfell et al., 2007a), which has to be taken into account in the analysis and interpretation of such spectra. Also, as the habitability of M star planets may be affected, future observation campaigns should ensure that enough non-M stars are in the sample to maximise the likelihood of a positive detection.

## Acknowledgments

This study was supported by the International Space Science Institute (ISSI) and benefited from the ISSI Team “Evolution of Exoplanet Atmospheres and their Characterisation.” J.L. Grenfell and H. Lammer acknowledge the Helmholtz-Gemeinschaft as this study was also carried out within the framework of the Helmholtz research project “Planetenentwicklung und Leben: Die Suche nach Leben im Sonnensystem und darüber hinaus.” We would also like to thank the referees for their comments and suggestions which helped to improve the paper.

## References

- Beaulieu, J.-P., Bennett, D.P., Fouqué, P., Williams, A., Dominik, M., Jorgensen, U.G., Kubas, D., Cassan, A., Coutuers, C., Greenhill, J., Hill, K., Menzies, J., Sackett, P.D., Albrow, M., Brilliant, S., Caldwell, J.A.R., Calitz, J.J., Cook, K.H., Corrales, E., Desort, M., Dieters, S., Dominis, D., Donatowicz, J., Hoffman, M., Kane, S., Marquette, J.-B., Martin, R., Meintjes, P., Pollard, K., Sahu, K., Vinter, C., Wambsgans, J., Woller, K., Horne, K., Steele, I., Bramich, D.M., Burgdorf, M., Snodgrass, C., Bode, M., Udalski, A., Szymański, M.K., Kubiak, M., Więckowski, T., Pietrzyński, G., Soszyński, I., Szewczyk, O., Wyrzykowski, Ł., Paczyński, B., Abe, F., Bond, I.A., Britton, T.R., Gilmore, A.C., Hearnshaw, J.B., Itow, Y., Kamiya, K., Kilmartin, P.M., Korpela, A.V., Masuda, K., Matsubara, Y., Motomura, M., Muraki, Y., Nakamura, S., Okada, C., Ohnishi, K., Rattenbury, N.J., Sako, T., Sato, S., Sasaki, M., Sekiguchi, T., Sullivan, D.J., Tristram, P.J., Yock, P.C.M., Yoshioka, T., 2006. Discovery of a cool planet at 5.5 Earth masses through gravitational microlensing. *Nature* 439, 437–440.
- Belisheva, N.K., Kuzhevskii, B.M., Vashenyuk, E.V., Zhiron, V.K., 2005. Correlation between the fusion dynamics of cells growing *in vitro* and variations of neutron intensity near the Earth's surface. *Dokl. Biochem. Biophys.* 402, 254–257.
- Buccino, A.P., Lemarchand, G.A., Mauas, P.J.D., 2007. UV habitable zones around M stars. *Icarus* 192, 582–587.
- Correia, A.C.M., Laskar, J., 2003. Different tidal torques on a planet with a dense atmosphere and consequences to the spin dynamics. *J. Geophys. Res.* 108 (E11), doi:10.1029/2003JE002059. 9-1–9-10.
- Crutzen, P.J., 1970. The influence of nitrogen oxides on the atmospheric ozone content. *Q. J. R. Meteorol. Soc.* 96, 320–325.
- Fichtner, H., 2001. Anomalous cosmic rays: Messengers from the outer heliosphere. *Space Sci. Rev.* 95, 639–754.
- Fridlund, C.V.M., 2004. The Darwin mission. *Adv. Space Res.* 34, 613–617.
- Goldreich, P., Soter, S., 1966. Q in the Solar System. *Icarus* 5, 375–389.
- Grenfell, J.L., Grießmeier, J.-M., Patzer, B., Rauer, H., Segura, A., Stadelmann, A., Stracke, B., Titz, R., von Paris, P., 2007a. Biomarker response to galactic cosmic ray-induced NO<sub>x</sub> and the methane greenhouse effect in the atmosphere of an earthlike planet orbiting an M dwarf star. *Astrobiology* 7 (1), 208–221.
- Grenfell, J.L., Stracke, B., von Paris, P., Patzer, B., Titz, R., Segura, A., Rauer, H., 2007b. The response of atmospheric chemistry on earthlike planets around F, G and K stars to small variations in orbital distance. *Planet. Space Sci.* 55, 661–671.
- Grenfell, J.L., Grießmeier, J.-M., Patzer, B., Rauer, H., Stracke, B., von Paris, P., 2008. Response of atmospheric biomarkers and related molecules to NO<sub>x</sub> generated by stellar cosmic rays for planets in the habitable zone of active M-dwarf stars, to be submitted for publication.
- Grießmeier, J.-M., 2006. Aspects of the magnetosphere–stellar wind interaction of close-in extrasolar planets. Ph.D. thesis, Technische Universität Braunschweig, ISBN 3-936586-49-7, Copernicus-GmbH, Katlenburg-Lindau, URL: <http://www.digibib.tu-bs.de/?docid=00013336>.
- Grießmeier, J.-M., Stadelmann, A., Penz, T., Lammer, H., Selsis, F., Ribas, I., Guinan, E.F., Motschmann, U., Biernat, H.K., Weiss, W.W., 2004. The effect of tidal locking on the magnetospheric and atmospheric evolution of Hot Jupiters. *Astron. Astrophys.* 425, 753–762.
- Grießmeier, J.-M., Stadelmann, A., Lammer, H., Belisheva, N., Motschmann, U., 2005a. The impact of galactic cosmic rays on extrasolar Earth-like planets in close-in habitable zones. In: Favata, F., Sanz-Forcada, J., Giménez, A., Battrick, B. (Eds.), Proc. 39th ESLAB Symposium. ESA SP-588, pp. 305–309.
- Grießmeier, J.-M., Stadelmann, A., Motschmann, U., Belisheva, N.K., Lammer, H., Biernat, H.K., 2005b. Cosmic ray impact on extrasolar Earth-like planets in close-in habitable zones. *Astrobiology* 5 (5), 587–603.
- Grießmeier, J.-M., Zarka, P., Spreuw, H., 2007. Predicting low-frequency radio fluxes of known extrasolar planets. *Astron. Astrophys.* 475, 359–368.
- Haagen-Smit, A., 1952. Chemistry and physiology of Los Angeles smog. *Ind. Eng. Chem.* 44, 1342–1346.
- Heath, M.J., Doyle, L.R., Joshi, M.M., Haberle, R.M., 1999. Habitability of planets around red dwarf stars. *Origins Life Evol. Biosphere* 29, 405–424.
- Heber, B., Fichtner, H., Scherer, K., 2006. Solar and heliospheric modulation of galactic cosmic rays. *Space Sci. Rev.* 125, 81–93.
- Holzwarth, V., Jardine, M., 2007. Theoretical mass loss rates of cool main-sequence stars. *Astron. Astrophys.* 463, 11–21.
- Hubbard, W.B., 1984. *Planetary Interiors*. Van Nostrand Reinhold Co., New York.
- Joshi, M., 2003. Climate model studies of synchronously rotating planets. *Astrobiology* 3 (2), 415–427.
- Joshi, M.M., Haberle, R.M., Reynolds, R.T., 1997. Simulations of the atmospheres of synchronously rotating terrestrial planets orbiting M dwarfs: Conditions for atmospheric collapse and the implications for habitability. *Icarus* 129, 450–465.
- Kallenrode, M.-B., 2000. Galactic cosmic rays. In: Scherer, K., Fichtner, H., Marsch, E. (Eds.), *The Outer Heliosphere: Beyond the Planets*. Copernicus Ges., Katlenburg-Lindau, chap. 7, pp. 165–190.
- Kasting, J.F., Whitmire, D.P., Reynolds, R.T., 1993. Habitable zones around main sequence stars. *Icarus* 101, 108–128.
- Khodachenko, M.L., Ribas, I., Lammer, H., Grießmeier, J.-M., Leitner, M., Selsis, F., Eiroa, C., Hanslmeier, A., Biernat, H.K., Farrugia, C.J., Rucker, H.O., 2007. Coronal Mass Ejection (CME) activity of low mass M stars as an important factor for the habitability of terrestrial exoplanets. I. CME impact on expected magnetospheres of Earth-like exoplanets in close-in habitable zones. *Astrobiology* 7 (1), 167–184.
- Kuchner, M.J., 2003. Volatile-rich Earth-mass planets in the habitable zone. *Astrophys. J.* 596, L105–L108.
- Lammer, H., Lichtenegger, H.I.M., Kulikov, Y.N., Grießmeier, J.-M., Terada, N., Erkaev, N.V., Biernat, H.K., Khodachenko, M.L., Ribas, I., Penz, T., Selsis, F., 2007. Coronal Mass Ejection (CME) activity of low mass M stars as an important factor for the habitability of terrestrial exoplanets. II. CME induced ion pick up of Earth-like exoplanets in close-in habitable zones. *Astrobiology* 7 (1), 185–207.
- Lammer, H., Khodachenko, M.L., Lichtenegger, H.I.M., Kulikov, Y.N., 2008. Impact of stellar activity on the evolution of planetary atmospheres and habitability. In: Dvorak, R. (Ed.), *Extrasolar Planets: Formation, Detection and Dynamics*. Wiley-VCH, Berlin.
- Léger, A., Selsis, F., Sotin, C., Guillot, T., Despois, D., Mawet, D., Ollivier, M., Labèque, F.A., Brachet, C.V., Chazelas, B., Lammer, H., 2004. A new family of planets? “Ocean-Planets.” *Icarus* 169, 499–504.
- Lestrade, J.-F., Wyatt, M.C., Bertoldi, F., Dent, W.R.F., Menten, K.M., 2006. Search for cold debris disks around M-dwarfs. *Astron. Astrophys.* 460, 733–741.
- Lovelock, J.E., 1965. A physical basis for life detection experiments. *Nature* 207, 568–670.
- Lovis, C., Mayor, M., Pepe, F., Alibert, Y., Benz, W., Bouchy, F., Correia, A.C.M., Laskar, J., Mordasini, C., Queloz, D., Santos, N.C., Udry, S., Bertaux, J.-L., Sivan, J.-P., 2006. An extrasolar planetary system with three Neptune-mass planets. *Nature* 441, 305–309.
- MacDonald, G.J.F., 1964. Tidal friction. *Rev. Geophys.* 2 (3), 467–541.
- Mann, G., Jansen, F., MacDowall, R.J., Kaiser, M.L., Stone, R.G., 1999. A heliospheric model and type III radio bursts. *Astron. Astrophys.* 348, 614–620.
- McDonald, F.B., Moraal, H., Reinecke, J.P.L., Lal, N., McGuire, R.E., 1992. The cosmic radiation in the heliosphere at successive solar minima. *J. Geophys. Res.* 97 (A2), 1557–1570.
- Murray, C.D., Dermott, S.F., 1999. *Solar System Dynamics*. Cambridge University Press, Cambridge.
- Parker, E.N., 1958. Dynamics of the interplanetary gas and magnetic fields. *Astrophys. J.* 128, 664–676.
- Peale, S.J., 1999. Origin and evolution of the natural satellites. *Annu. Rev. Astron. Astrophys.* 37, 533–602.
- Prössl, G.W., 2004. *Physics of the Earth's Space Environment*. Springer-Verlag, Berlin.
- Reeves, G.D., Cayton, T.E., Gary, S.P., Belian, R.D., 1992. The great solar energetic particle events of 1989 observed from geosynchronous orbit. *J. Geophys. Res.* 97 (A5), 6219–6226.
- Ribas, I., Font-Ribera, A., Beaulieu, J.-P., 2008. A  $\sim 5M_{\oplus}$  super-Earth orbiting GJ 436? The world of near-grazing transits. *Astrophys. J.* 677, L59–L62.
- Rivera, E.J., Lissauer, J.J., Butler, R.P., Marcy, G.W., Vogt, S.S., Fischer, D.A., Brown, T.M., Laughlin, G., Henry, G.W., 2005. A  $\sim 7.5M_{\oplus}$  planet orbiting the nearby star, GJ 876. *Astrophys. J.* 634, 625–640.
- Sagan, C., Thomson, W.R., Carlson, R., Gurnett, D., Hord, C., 1993. A search for life on Earth from the Galileo spacecraft. *Nature* 365, 715–721.
- Scalo, J., Kaltenegger, L., Segura, A., Fridlund, M., Ribas, I., Kulikov, Y.N., Grenfell, J.L., Rauer, H., Odert, P., Leitzinger, M., Selsis, F., Khodachenko, M.L., Eiroa, C., Kasting, J., Lammer, H., 2007. M stars as targets for terrestrial exoplanet searches and biosignature detection. *Astrobiology* 7 (1), 85–166.
- Scherer, K., Fichtner, H., Heber, B., Ferreira, S.E.S., Potgieter, M.S., 2008. Cosmic ray flux at the Earth in a variable heliosphere. *Adv. Space Res.* 41, 1171–1176.
- Schindler, T.L., Kasting, J.F., 2000. Synthetic spectra of simulated terrestrial atmospheres containing possible biomarker gases. *Icarus* 145, 262–271.
- Schneider, J., Riadu, P., Tinetti, G., Schmid, H.M., Stam, D., Udry, S., Baudoz, P., Boccaletti, A., Grasset, O., Mawet, D., Surdej, J., The See-Coast Team, 2006. SEE-COAST: The Super-Earth Explorer. In: Barret, D., Casoli, F., Contini, T., Lagache, G., Levacelier, A., Pagani, L. (Eds.), SF2A-2006: Semaine de l'Astrophysique Française, pp. 429–432.
- Selsis, F., 2004. The atmosphere of terrestrial exoplanets: Detection and characterisation. In: Beaulieu, J.-P., Lecavelier des Etangs, A., Terquem, C. (Eds.), *Extrasolar Planets, Today and Tomorrow*. In: ASP Conf. Ser., vol. 321, pp. 170–181.
- Selsis, F., Despois, D., Parisot, J.-P., 2002. Signature of life on exoplanets: Can Darwin produce false positive detections? *Astron. Astrophys.* 388, 985–1003.

- Selsis, F., Chazelas, B., Bordé, P., Ollivier, M., Brachet, F., Decaudin, M., Bouchy, F., Ehrenreich, D., Grießmeier, J.-M., Lammer, H., Sotin, C., Grasset, O., Moutou, C., Barge, P., Deleuil, M., Mawet, D., Despois, D., Kasting, J.F., Léger, A., 2007. Could we identify hot ocean-planets with CoRoT, Kepler and Doppler velocimetry? *Icarus* 191, 453–468.
- Seo, E.S., McDonald, F.B., Lal, N., Webber, W.R., 1994. Study of cosmic-ray H and He isotopes at 23 AU. *Astrophys. J.* 432, 656–664.
- Shea, M.A., Smart, D.F., 2000. Cosmic ray implications for human health. *Space Sci. Rev.* 93, 187–205.
- Smart, D.F., Shea, M.A., Flückiger, E.O., 2000. Magnetospheric models and trajectory computations. *Space Sci. Rev.* 93, 305–333.
- Smith, D.S., Scalo, J., Wheeler, J.C., 2004. Transport of ionising radiation in terrestrial-like exoplanet atmospheres. *Icarus* 171, 229–253.
- Stadelmann, A., 2005. Globale Effekte einer Erdmagnetfeldumkehrung: Magnetosphärenstruktur und kosmische Teilchen. Ph.D. thesis, Technische Universität Braunschweig, ISBN 3-936586-42-X, Copernicus-GmbH, Katlenburg-Lindau, URL: <http://www.digibib.tu-bs.de/?docid=00000002>.
- Tarter, J.C., Backus, P.R., Mancinelli, R.L., Aurnou, J.M., Backman, D.E., Basri, G.S., Boss, A.P., Clarke, A., Deming, D., Doyle, L.R., Feigelson, E.D., Freund, F., Grinspoon, D.H., Haberle, R.M., Hauck II, S.A., Heath, M.J., Henry, T.J., Hollingsworth, J.L., Joshi, M.M., Kilston, S., Liu, M.C., Meikle, E., Reid, I.N., Rothschild, L.J., Scalo, J., Segura, A., Tang, C.M., Tiedje, J.M., Turnbull, M.C., Walkowicz, L.M., Weber, A.L., Young, R.E., 2007. A reappraisal of the habitability of planets around M dwarf stars. *Astrobiology* 7 (1), 30–65.
- Udry, S., Bonfils, X., Delfosse, X., Forveille, T., Mayor, M., Perrier, C., Bouchy, F., Lovis, C., Pepe, F., Queloz, D., Bertaux, J.-L., 2007. The HARPS search for southern extra-solar planets. XI. Super-Earths (5 and 8  $M_{\oplus}$ ) in a 3-planet system. *Astron. Astrophys.* 469, L43–L47.
- Valencia, D., O'Connell, R.J., Sasselov, D., 2006. Internal structure of massive terrestrial planets. *Icarus* 181, 545–554.
- Valencia, D., Sasselov, D.D., O'Connell, R.J., 2007. Detailed models of super-Earths: How well can we infer bulk properties? *Astrophys. J.* 665, 1413–1420.
- Vogt, J., Zieger, B., Glassmeier, K.-H., Stadelmann, A., Kallenrode, M.-B., Sinnhuber, M., Winkler, W., 2007. Energetic particles in the paleomagnetosphere: Reduced dipole configurations and quadrupolar contributions. *J. Geophys. Res.* 112 (A11), A06216.
- Voigt, G.-H., 1981. A mathematical magnetospheric field model with independent physical parameters. *Planet. Space Sci.* 29, 1–20.
- Voigt, G.-H., 1995. Magnetospheric configuration. In: Volland, H. (Ed.), *Handbook of Atmospheric Electrodynamics*, vol. II. CRC Press, Boca Raton, chap. 11, pp. 333–388.
- Wood, B.E., Müller, H.-R., Zank, G.P., Linsky, J.L., 2002. Measured mass-loss rates of solar-like stars as a function of age and activity. *Astrophys. J.* 574, 412–425.
- Wood, B.E., Müller, H.-R., Zank, G.P., Linsky, J.L., Redfield, S., 2005. New mass-loss measurements from astrospheric Ly $\alpha$  absorption. *Astrophys. J.* 628, L143–L146.